Precise Upright Adjustment of Panoramic Images

Nobuyuki Kita
TICO-AIST Cooperative Research Laboratory for Advanced Logistics (ALLAB),
National Institute of Advanced Industrial Science and Technology (AIST), Tsukuba, Japan

Keywords: Panoramic, Equirectangular, Upright Adjustment, Vertical Lines, Omnidirectional, 360 Degree, Spherical.

Abstract: An equirectangular format is often used when an omnidirectional image taken by a 360° camera is expanded into a single image, which is referred to as a panoramic image. If an omnidirectional image is expanded into a panoramic image using the upward direction of the inclined camera, the image may look unstable and "wavy." It is important to correct the inclination using the zenith direction as a reference; this task is called "upright adjustment." In this paper, we propose a method for upright adjustment by estimating the inclination of a camera in a wavy panoramic image using vertical lines in the environment, e.g., indoors or outdoors near a building. The advantage of the proposed method is that 3D straight lines are detected with high accuracy and high speed directly from a panoramic image without passing through a spherical image. Experimental results of upright adjustment of the wavy panoramic images taken in multiple places show that the proposed method is accurate and can be applied in a wide range of indoor and outdoor scenarios.

1 INTRODUCTION

Many 360° cameras are on the market, and it has become easy to obtain omnidirectional images, which are used for applications such as personal and SNS viewing, VR use, and real-estate advertisement (Ricoh 2020). In the 1980s, in robotics and related fields, omnidirectional cameras were made by hand. The estimation of self-position and posture as well as three-dimensional (3D) reconstruction of the environment were carried out using these images (Yagi 1999). At present, research using a lightweight, high-resolution commercial 360° camera for mobile-robot vision is ongoing (Payá, Gil et al. 2017; Jayasuriya, Ranasinghe et al. 2020).

An omnidirectional image may be regarded as a storage of color (or intensity) information in the whole viewing direction from the origin, and it is expanded into various 2D formats and projected on a display device or printed according to the application. For example, when the information is displayed on an HMD for VR, partial information about the viewing direction is converted into a perspective projection and displayed on the HMD.

When information in all directions is displayed in one image, it is necessary to expand a sphere into a plane, and a common method is to expand the sphere to an equirectangular format, which is referred to as a panoramic image. In Figure 1(a), the image is constructed using the upward direction of the inclined camera, and the image looks unstable and "wavy." In contrast, Figure 1(b) is a panoramic image

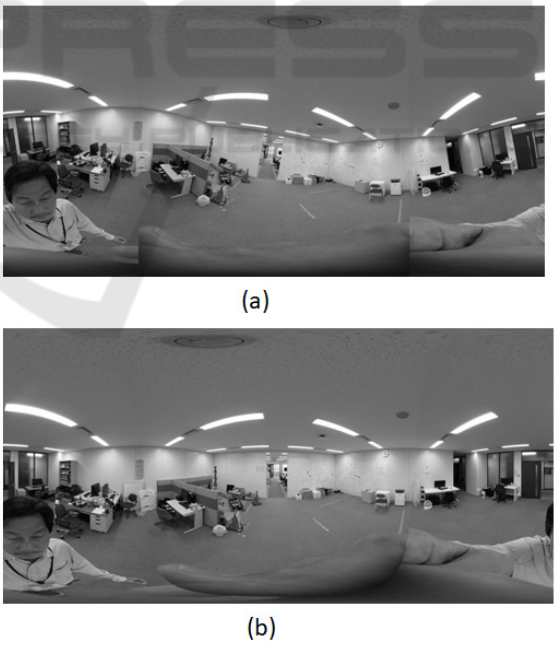

Figure 1: Example of a panoramic image before and after inclination correction.

Kita, N.
Precise Upright Adjustment of Panoramic Images.
DOI: 10.5220/0010242600990111
In *Proceedings of the 16th International Joint Conference on Computer Vision, Imaging and Computer Graphics Theory and Applications (VISIGRAPP 2021) - Volume 4: VISAPP*, pages 99-111
ISBN: 978-989-758-488-6

constructed using the zenith direction obtained by knowing the inclination of the camera at the time of image capture.

Even when directly viewing an omnidirectional image with an HMD or similar device, if the camera inclination is not corrected, an image with an inclination that does not match that of the HMD is displayed, so inclination correction is important. Therefore, many studies have investigated image display in VR without discomfort (Jung, Kim et al. 2017; Jeon, Jung et al. 2018; Jung, Lee et al. 2019).

When omnidirectional images are used for the vision of mobile robots such as AGVs and UAVs, many studies convert them into panoramic images. For AGV applications, many studies use yaw as the only camera pose degree of freedom (DOF) (Milford and Wyeth 2010; Liu, Pradalier et al. 2013). In contrast, in UAVs, the camera posture has three DOFs, and the roll and pitch of the camera must be estimated (Demonceaux, Vasseur et al. 2007; Natraj, Ly et al. 2013). Even in an AGV, three DOFs of the camera attitude must be considered to enable the application to handle running surfaces that are not flat (Bosse, Rikoski et al. 2002). If the camera tilt is estimated and an inclination corrected panoramic image is obtained, a method using yaw only can be employed. However, the inclination correction must be more accurate than that required in VR.

The accuracy of inclination correction depends on the accuracy of camera inclination estimation at the time of image capture. Some methods use information from external sensors such as IMUs, whereas others use image analysis to determine the zenith direction. The latter approach can be further divided into methods that utilize vertical or horizontal lines in the environment and those that do not.

In this paper, we use longitudinally parallel lines existing in the environment without the help of an external sensor. Many methods have been proposed for estimating the inclination of a camera by detecting straight lines in the environment using a omnidirectional image as input. However, most detect 3D straight lines by detecting the great circles on a spherical image, and no research has detected straight lines in the environment directly from a panoramic image. Here, 3D straight lines in the longitudinal direction are directly detected from the panoramic image before correction, and the azimuth and inclination angle are estimated with high accuracy. For this purpose, a method of performing a special Hough transform of an edge point on a panoramic image is analytically derived. Next, a method for selecting parallel lines from the detected 3D lines is obtained analytically. Moreover, it is shown that the inclination in the camera coordinate system of the parallel lines can be obtained. Unless it is a special environment, a longitudinally parallel line group is a vertical line group, and this is the zenith direction. Thus, we obtain fast and accurate method for correcting the inclination of the camera.

The contributions of this paper are as follows.

- A formula for the curve on a panoramic image of a longitudinal 3D line in the environment is derived.
- A special Hough transform of the edge points in the longitudinal direction based on the derived equation realizes stable 3D line detection.
- The constraints of the projected image of a group of longitudinal straight lines are obtained analytically.
- The inclination of the camera is estimated robustly and accurately by RANSAC (Fischler, Martin et al. 1981) processing based on the constraints.

Section 2 reviews existing research on camera tilt correction, Section 3 explains the proposed method, Section 4 describes the implementation including speedup, and Section 5 analyzes the experimental results. Section 6 discusses differences between this work and similar studies, and Section 7 concludes with a discussion of future work.

2 RELATED WORK

Studies have been conducted for many years to estimate the inclination of a camera at the time of image capture by analyzing the image itself to generate an image with the correct inclination (Cipolla, Robertson et al. 1999; Gallagher 2005; Lee, Shechtman et al. 2013). Lee et al. (2013) call this "upright adjustment," and we follow their lead. The methods for upright adjustment can be divided into two groups: methods that do and do not use the vertical and horizontal lines in the environment. In this section, we focus on studies that use omnidirectional images as input.

2.1 Methods using 3D Lines

Based on the Manhattan world assumptions (Coughlan and Yuille 1999; Zhang, Lu et al. 2016) and the Atlanta world assumptions (Schindler and Dellaert 2004; Joo, Oh et al. 2018), which state that a group of parallel lines existing indoors or in the suburbs is generally a group of vertical lines or a group of horizontal lines, many studies have been conducted to estimate the inclination of a camera by

detecting a vanishing point from a projection image of a group of lines.

Wang et al. (2003) projected an omnidirectional image onto a unit sphere, detected the edge points and their slopes, voted for a straight line cutting Z = 1 for each edge point, and the position of the peak score was considered the zenith direction.

Using the orthogonality of multiple vanishing points as a constraint, Bazin et al. (2012) stably detected the vanishing points of parallel line groups in the environment. These groups are based on the detection of the great circle on the unit sphere for individual straight line detection.

Jung et al. (2017) converted a panoramic image into a Cubemap to detect straight line segments. After separating the lines into horizontal and vertical directions using the Hough transform of the line-segment end points in spherical coordinates with the line-segment length as a weight, they find the great circles in the horizontal and vertical directions. Next, the intersection of the great circle in the horizontal direction is obtained as a vector to the horizontal vanishing point. The vector to the zenith direction is estimated by orthogonality to the normal vector of the great circle in the vertical direction and the vector to the horizontal vanishing point. Since they use both vertical and horizontal lines in the environment, the estimation can be obtained even if there are no vertical lines in the environment. Since a great circle detected on the basis of both ends of the short line segment contains considerable error, repetition is required to reduce the inclination estimation error.

Kawai (2019) corrected the inclination of the camera based on the knowledge that the projection image of the 3D vertical line on the panoramic image can be detected as a line segment in the direction slightly inclined from the vertical near the vertical center line of the image. Moreover, the relationship between the horizontal position intersecting the vertical center line of the image and the tilt can be approximated by a sine wave, which yields the inclination of a camera.

2.2 Methods Not using 3D Lines

In (Demonceaux, Vasseur et al. 2006), to detect the attitude of a UAV, a horizontal line was detected by separating the omnidirectional image into sky/ground; the inclination of the camera was the direction perpendicular to the horizontal line.

Jung et al. (2019) proposed a method using deep learning without using a group of straight lines or a horizontal line. From the SUN360 dataset (Xiao, Ehinger et al. 2012), which consists of 67,000 upright panoramic images of various scenes, panoramic images appropriately inclined in an arbitrary direction were synthesized through spherical projection. Three kinds of CNNs were trained using these images, and the results were compared. The average estimation error was 5°.

Jeon et al. (2018) derived the relationship between the 2D rotation of a small rectangular area near the vertical center lines of the panoramic image and the 3D rotation of the camera. They further derived the periodic relationship between the amount of 2D rotation and lateral position. The 2D rotation of the small region was estimated by a trained CNN, and the 3D tilt of the camera was estimated by the RANSAC method with the periodic function as a constraint. An average error of 1.3°, including cases without straight or horizontal lines, was achieved experimentally.

3 UPRIGHT ADJUSTMENT METHOD

The proposed method detects a group of longitudinal 3D straight lines from a panoramic image taken indoors or outdoors adjacent to a structure and estimates the inclination of the camera. In similar methods, a 3D straight line is detected as a great circle after conversion into a spherical projection, but in this method, a 3D straight line is detected with high accuracy directly from a panoramic image. For this purpose, a new Hough transform is proposed.

3.1 Coordinate System Definitions

Figure 2(a) shows an omnidirectional camera coordinate system OXYZ and a panoramic projection cylinder, and Figure 2(b) shows a panoramic coordinate system $O_p\omega\varphi$ and a panoramic image coordinate system O_iuv. The panoramic projection plane is a cylindrical plane with the camera Z axis as a central axis, and a point in 3D space P' is projected onto a point $P(X_p, Y_p, Z_p)$ on the cylindrical plane. For convenience, the radius of the cylindrical surface is 1. Then, ${X_p}^2 + {Y_p}^2 = 1$ and $-\infty < Z_p < \infty$.

The cylindrical surface is cut in a direction parallel to the Z axis and expanded in a 2D plane to form the panoramic coordinate system. For convenience, if the cut position is along the negative X axis, the origin of panoramic coordinate system O_p is position ${O_p}'$, where the cylindrical surface and the X-axis intersect. Moreover, horizontal axis ω is a horizontal distance on the cylindrical surface from

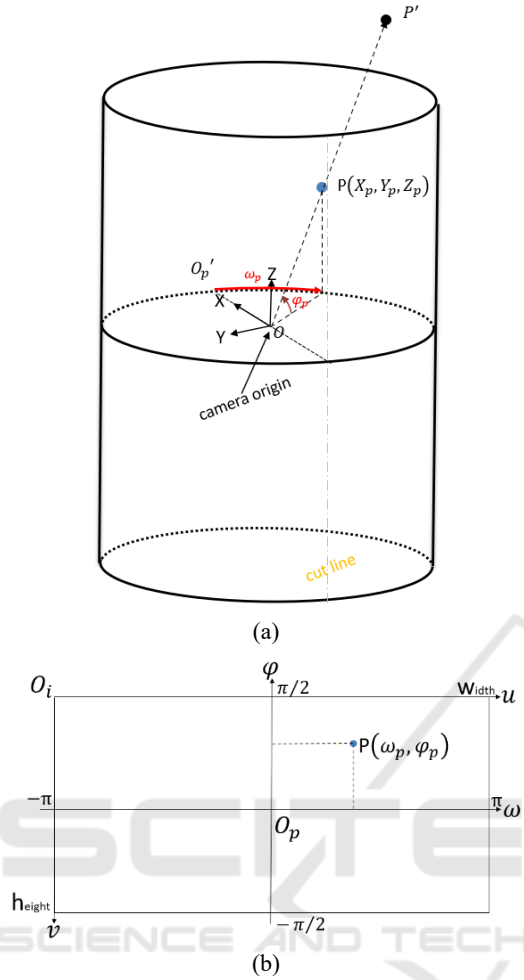

Figure 2: (a) Omnidirectional camera coordinate system OXYZ and a panoramic projection cylinder. (b) Panoramic coordinate system $O_p\omega\varphi$ and panoramic image coordinate system O_iuv.

$O_p{}'$ and indicates an azimuth angle, $-\pi < \omega < \pi$. Vertical axis ϕ of the panoramic coordinate system corresponds to the elevation angle in the camera coordinate system, $-\pi/2 < \phi < \pi/2$.

The relationship between the panoramic image coordinates (u, v) and panoramic coordinates (ω, φ) is as follows for an image *width* × *height* in size:

$$\omega = (u - width/2 + 0.5) \times 2\pi/width$$

$$\varphi = (height/2 - v + 0.5) \times \pi/height$$

3.2 Basic Principles

As shown in Figure 3, the projection curve of a longitudinal 3D straight line on the cylindrical surface is a part of the outline of the cross section in which

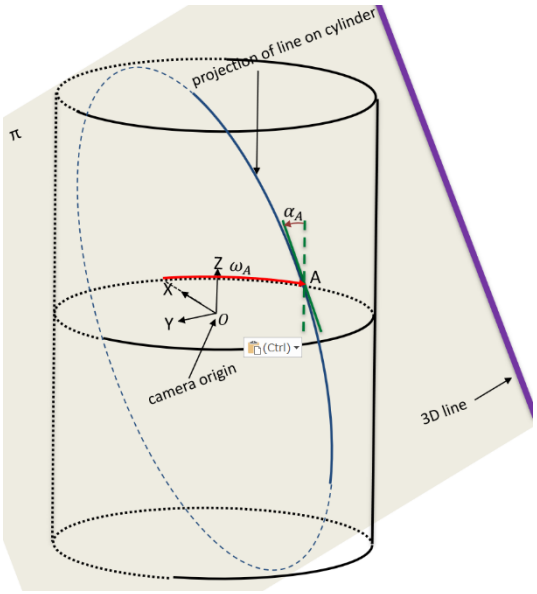

Figure 3: Projection curve of the longitudinal 3D straight line on the cylindrical surface.

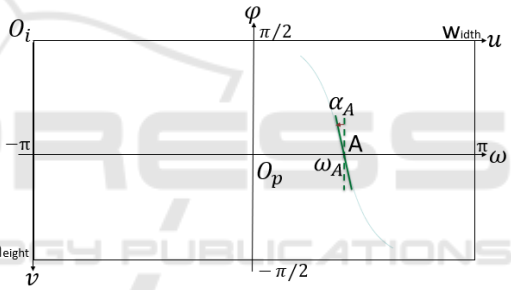

Figure 4: ω_A and α_A on the panoramic image.

the 3D plane π including the camera center and the 3D straight line cuts the cylinder (blue solid line in Figure 3).

Let the point where the projection curve on the cylindrical surface intersects the XY plane (Z = 0) be A, the azimuth angle be ω_A, and the inclination from the Z axis of the tangent of the projection curve at point A be α_A. It can be seen that the plane π including the 3D straight line is inclined by α_A degrees around $\overline{OA}$ which is the vector indicating the azimuth angle ω_A.

Figure 4 shows ω_A and α_A on a panoramic image. The blue curved line is a 2D projection curve obtained by developing a 3D projection curve on a cylindrical surface onto a panoramic image. Here, the intersection point with the ω axis is A, ω_A is obtained as the azimuth angle of point A, and α_A is obtained as the angle between a tangent of the 2D projection curve at point A and the ϕ axis.

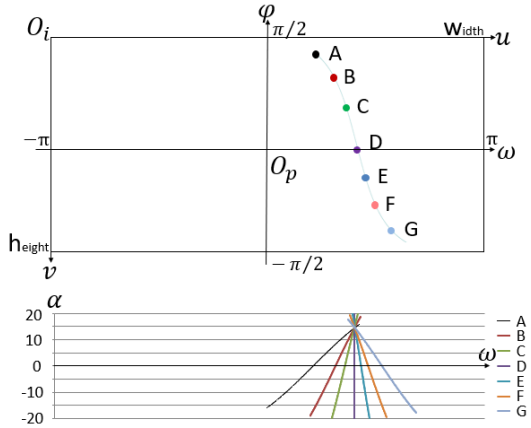

Figure 5: Example of special Hough transform.

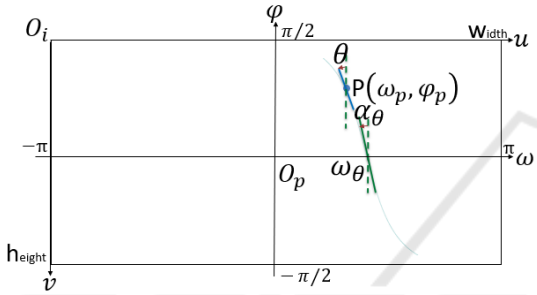

Figure 6: ($\omega\theta$,$\alpha\theta$) must be obtained from P(ωP,αP) and θ.

That is, if (ω, α) can be detected for a 2D projection curve of a 3D straight line on a panoramic image, the inclination or normal direction of the 3D plane π including the 3D straight line can be obtained.

If two parallel lines exist in the 3D space and (ω, α) can be obtained for each of the projected curves on the panoramic image, the direction vector of the parallel line is a vector orthogonal to the normal direction of the two 3D planes.

3.3 Detection of a 3D Straight Line from a Panoramic Image

The detection of 3D straight lines from a projected image generally consists of two steps. First, edge points are detected on the image by an edge detector such as Canny (Canny, John 1986). Next, 3D lines are detected by grouping the edge points in the parameter space by a Hough transform or the like.

For a perspective projection image, since a projection of a 3D straight line is a 2D straight line, it can be obtained by a Hough transform in which the straight line of every inclination passing through the edge point is voted in a parameter space (ρ, θ)

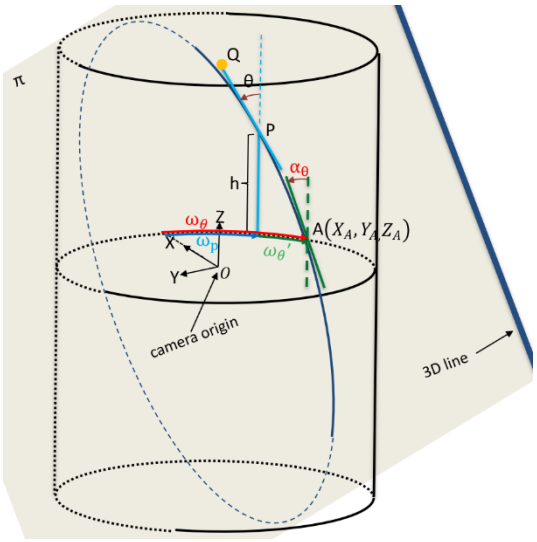

Figure 7: $(\omega_\theta, \alpha_\theta)$ from P and θ in the camera coordinate system.

representing the straight line (Illingworth, John et al. 1988).

In the case of a panoramic image, as shown in Figure 4, the projection of a 3D straight line is a curve, and we represent this curve by one set of ω and α. Then, a 3D straight line is detected by the Hough transform, which votes in the (ω, α) space with respect to the projection curve of every inclination passing through the edge point detected on the panoramic image. Figure 5 shows an example of such a Hough transform. Each of the edge points A from G on the panoramic image is converted to a curved line in the parameter space. Thus, when the edge points lie on the projection curve of a 3D straight line, many votes are collected at one point on the parameter space. To do this, as shown in Figure 6, it is necessary to obtain $(\omega_\theta, \alpha_\theta)$ when the projection curve passes through edge point P(ω_P, α_P) with an inclination of θ °.

We derive the calculation of $(\omega_\theta, \alpha_\theta)$ from (ω_P, α_P) and θ in the camera coordinate system, as shown in Figure 7. Edge point P is located at azimuth ω_p and height $\mathrm{h} = \tan\varphi_p$ on the panoramic cylindrical surface. Note that $\omega_\theta = \omega_p + \omega_\theta{}'$ and only $\omega_\theta{}'$ depends on h and θ. Hereafter, it is assumed that edge point P is in the X-axis direction, that is, $\omega_P = 0$. The coordinates of point P in the camera coordinate system are (1, 0, h). Next, let a point on a straight line passing through an edge point P on the plane X = 1, where the angle formed by the Z axis is θ, be denoted by Q (1, tan θ, h + 1). Here, cutting plane π passes through the origin (0,0,0),

point P (1,0, h), and point Q (1, tan θ, h + 1). The equation of π is

$$hX + (1/\tan\theta)Y - Z = 0$$

The intersection between cutting plane π and the cylindrical surface is

$$X^2 + Y^2 = 1$$

and the X- and Y-coordinates are obtained by the following formulas using Z as a parameter.

$$X = \frac{h(\tan\theta)^2}{1 + h^2(\tan\theta)^2} Z \pm \frac{\sqrt{-(\tan\theta)^2 Z^2 + h^2(\tan\theta)^2 + 1}}{1 + h^2(\tan\theta)^2}$$

$$Y = \frac{\tan\theta}{1 + h^2(\tan\theta)^2} Z \pm \frac{\sqrt{-h^2(\tan\theta)^4 Z^2 + h^2(\tan\theta)^2(1 + h^2(\tan\theta)^2)}}{1 + h^2(\tan\theta)^2}$$

Let A (X_A, Y_A, Z_A) be the coordinates of a position where (ω, α) should be obtained when assuming $\omega_p = O$. Since $Z_A = 0$,

$$X_A = \pm\sqrt{\frac{1}{1 + h^2(\tan\theta)^2}}$$

$$Y_A = \pm\sqrt{\frac{h^2(\tan\theta)^2}{1 + h^2(\tan\theta)^2}}$$

Therefore, $\omega_\theta{}'$ in Figure 7 is

$$\omega_\theta{}' = \tan^{-1}\frac{Y_A}{X_A} = \tan^{-1}(h\tan\theta)$$

As for α_θ, because

$$\Delta X_A = \frac{\partial X}{\partial Z}(0) = \frac{h(\tan\theta)^2}{1 + h^2(\tan\theta)^2}$$

$$\Delta Y_A = \frac{\partial Y}{\partial Z}(0) = \frac{\tan\theta}{1 + h^2(\tan\theta)^2}$$

then

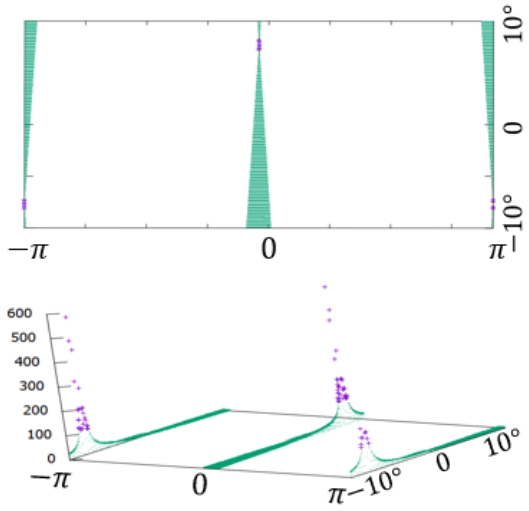

Figure 8: Voting result for the edge points on the projection curve when h = 0.0 and θ = 7.7°.

$$\alpha_\theta = \tan^{-1}\sqrt{\Delta X_A{}^2 + \Delta Y_A{}^2} = \tan^{-1}\frac{\tan\theta}{\sqrt{1 + h^2(\tan\theta)^2}}$$

Next, we have

$$\omega_\theta = \omega_p + \tan^{-1}(h\tan\theta) \quad (1)$$

$$\alpha_\theta = \tan^{-1}\frac{\tan\theta}{\sqrt{1 + h^2(\tan\theta)^2}} \quad (2)$$

When an edge point exists at coordinates (u, v) in the panoramic image coordinate system,

$$\mathrm{h} = \tan\big((height/2 - v + 0.5) \times \pi/height\big) \quad (3)$$

$$\omega_p = (u - width/2 + 0.5) \times 2\pi/width \quad (4)$$

Because $(\omega_\theta, \alpha_\theta)$ can be calculated by Equations (1)-(4) from (u, v) and θ, one vote is cast to the corresponding bin in (ω, α) space.

The range and granularity of (ω, α) and θ may be determined from the desired range and accuracy of the camera inclination estimation. The aim of the proposed method is to estimate camera inclination with high accuracy and the camera is assumed to incline in an arbitrary direction. Then the range of ω is $-\pi < \omega < \pi$ and ω is divided into the size of the image width. The upper limit of the camera inclination angle is set to 10° or 20° in this study, and the ranges of α and θ are divided into steps of 0.1°.

Figure 8 shows the voting result for the edge points on the projection curve when h = 0.0 and θ =

7.7°. A green dot indicates a bin with 1-99 votes, and a purple dot indicates a bin with >100 votes. The bin with the maximum in the purple region around $\omega = 0$ is $\alpha = 7.7^\circ$ at $\omega = 0.0^\circ$, and the bin with the maximum in the purple region around $\omega = -\pi$ is $\alpha = -7.7^\circ$ at $\omega = -\pi^\circ$. In other words, the azimuth and inclination degree of the 3D plane including a 3D longitudinal line can be detected with an accuracy of 0.1° or less by position (ω, α) at which the voting score is maximum within a region that exceeds a threshold value.

3.4 Robust Detection of Zenith Direction

As mentioned in Section 3.2, the inclination of a parallel 3D line in the camera coordinate system can be estimated if two 3D parallel lines can be detected in different directions from the viewpoint of the camera. However, there are some lines that are not parallel in the usual environment. In Section 3.3, (ω, α) of the projection curve is derived for a 3D straight line, but (ω, α) is also obtained for a straight line that is not parallel. Therefore, to correctly estimate the direction of the parallel 3D line group from the (ω, α) group detected from the panoramic image, the property of the projection curve of a parallel 3D line group is derived so that outliers can be eliminated.

As shown in Figure 9, when the azimuth and inclination angles of the parallel 3D line group in the camera coordinate system are φ and θ, respectively the coordinates of point Z are

$$\mathrm{Z} = (\sin\theta\cos\varphi, \sin\theta\sin\varphi, \cos\theta)$$

The 3D plane including each of the parallel lines and the camera origin rotates around OZ. Angle β at the position rotated by ω from the X direction is equal to the angle formed by OZ and OP with P being the position advanced by $\pi/2$ from ω. Here, the coordinates of P are

$$\mathrm{P} = (-\sin\omega, \cos\omega, 0)$$

Hence,

$$\beta = \cos^{-1}(Z \cdot P) = \cos^{-1}(\sin\theta\sin\varphi\cos\omega - \sin\theta\cos\varphi\sin\omega)$$

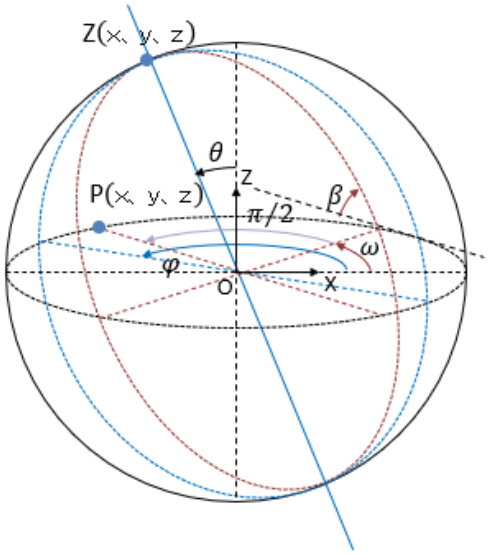

Figure 9: Property of the projection curve of a 3D parallel line group.

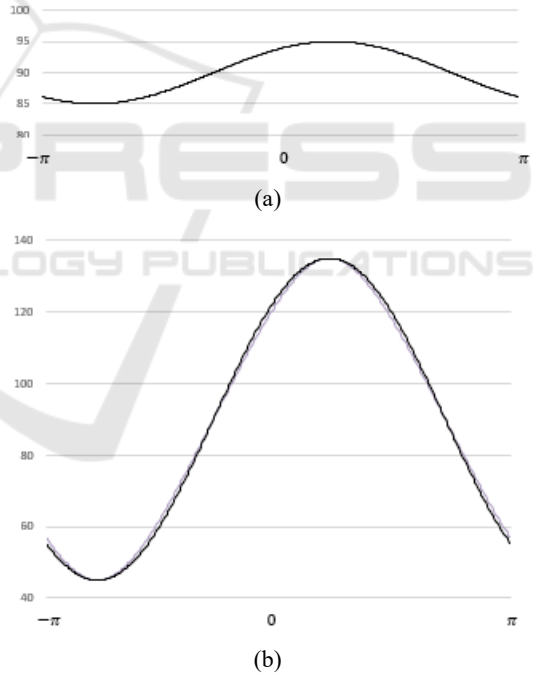

Figure 10: Curves when the azimuth angle is 130° and the inclination angle is (a) 5° and (b) 45°.

For example, Figure 10(a) shows the curve when the azimuth angle is 130° and the inclination angle is 5°. The curve is nearly equal to the curve

$$\beta = \theta \times \sin(\omega - \varphi) + \pi/2$$

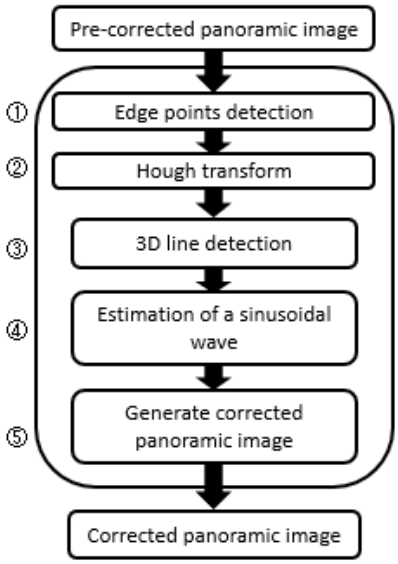

Figure 11: Proposed upright adjustment.

The absolute difference is not more than 0.003°. For larger inclination angles, when the azimuth angle is 130° and the inclination angle is 45°, Figure 10(b) shows the curve, and the maximum absolute difference is about 1.9°. However, there is no difference between the phase and amplitude. Here, because $\alpha = \pi / 2 - \beta$ of (ω, α), representing the projection image of the parallel 3D line, ω and α of the projection curve group of the parallel 3D line group on the panoramic image may be on a sine wave. Therefore, by applying the sinusoidal wave to the (ω, α) group detected from the panoramic image, the azimuth angle φ and inclination angle θ of the parallel straight line group can be obtained as the phases and amplitudes.

4 IMPLEMENTATIONS

Figure 11 shows a flow chart of the proposed process for upright adjustment.

First, a binary edge image is created from a panoramic image by the Canny function from OpenCV. Because the projection curve of a longitudinal 3D straight line has a direction close to the vertical except at the top and bottom of the panoramic image, even if the camera is tilted to some extent, the horizontal continuous edge points are removed.

Next, each edge point (u, v) is voted in (ω, α) space while changing θ. In this implementation, $-\pi < \omega < \pi$ is divided into *width* to handle the vertical and horizontal vibrations of the camera. The ranges of θ and α and step size are given by the parameters *maxangle* and *sampangle*, respectively, considering the desired range and accuracy of the camera tilt. In addition, because the upper area of a panoramic image is occupied by a ceiling and the sky and the lower area by a floor or road surface, only edge points within the parameter *vertarea* from the vertical center are considered. As Figure 4 shows, (ω', α) depends on h and θ but not on ω_P. Therefore, a conversion table from (h, θ) to (ω', α) is created in advance, and it is used to more quickly obtain (ω, α) from (u, v) and θ.

A 3D straight line is detected by determining the position with the maximum value in each column of a bin that has more votes than threshold *pthresh* in (ω, α) space. However, if there are consecutive maximum values in the column direction, only the position (ω, α) with the maximum number of votes is adopted. The (ω, α), obtained as described above, includes non-parallel lines. To perform a robust estimation, at the next RANSAC processing, a certain number of straight line candidates are required, and the threshold of the number of candidates is given by parameter *topthresh*. When a given *pthresh* may not yield more than *topthresh* line candidates, *pthresh* is reduced in increments of parameter *dec* until more than *topthresh* line candidates are obtained.

With respect to the set of (ω, α) greater than *topthresh*, *seednum* pieces are randomly selected to obtain a sinusoidal wave, and the candidates that deviate in the α direction from the sinusoidal wave less than parameter *thinlier* are processed by RANSAC as inliers, thereby robustly obtaining a sinusoidal wave.

The direction of the parallel straight line group is calculated from the phase and amplitude of the obtained sine wave, and the panoramic image is converted using this as the zenith direction. The inclination-corrected panoramic image is then output.

In addition, steps ② and ⑤ in Figure 11 were parallelized with OpenMP to increase speed.

5 EXPERIMENTAL RESULTS

5.1 Results of Upright Adjustment

Figures 12(a)–(f) show successful examples of upright adjustment. In each subfigure, the top row shows the panoramic image before correction. The next row shows the edge image in the considered

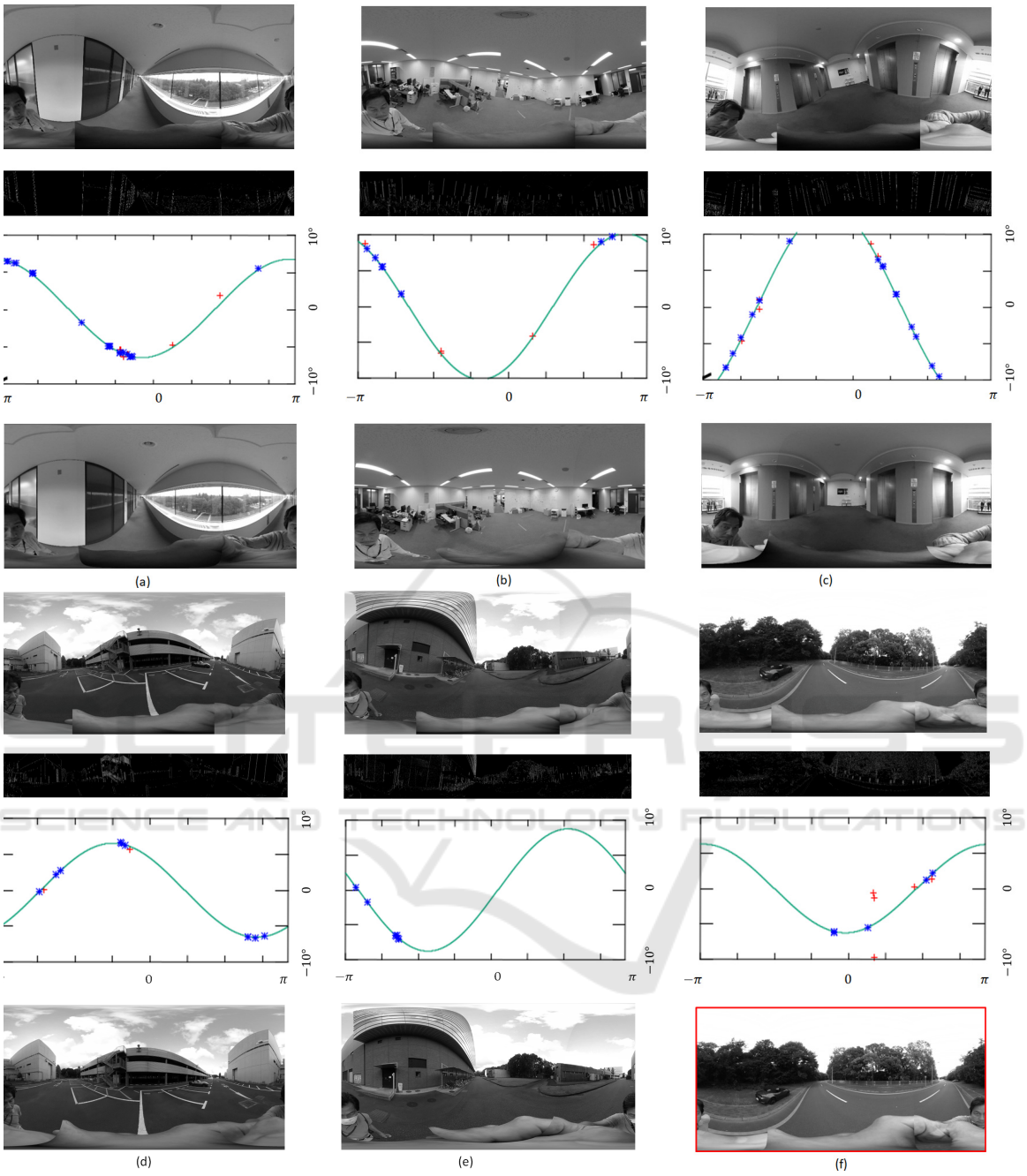

Figure 12: Successful examples of upright adjustment.

range, and the row below shows (ω, α) space, where blue indicates inliers, red indicates outliers, and the green line is the sine curve obtained by RANSAC. The bottom rows show the corrected panoramic image. The inputs were 3840 × 1920 panoramic images, Hough transformed with *maxangle* = 10.0, *sampangle* = 0.1, and *vertarea* = 300; detected with *pthresh* = 150, *topthresh* = 10, and *dec* = 10; and corrected based on the phase and amplitudes of the sinusoidal waves obtained by RANSAC with *seednum* = 3 and *thinlier* = 2.

Because Figure 12(a) shows a corridor and a large number of vertical lines exist near the camera, the upright adjustment can be performed stably. Figure 12(b) shows an image from the center of a room, in which the 3D vertical lines on the wall are projected

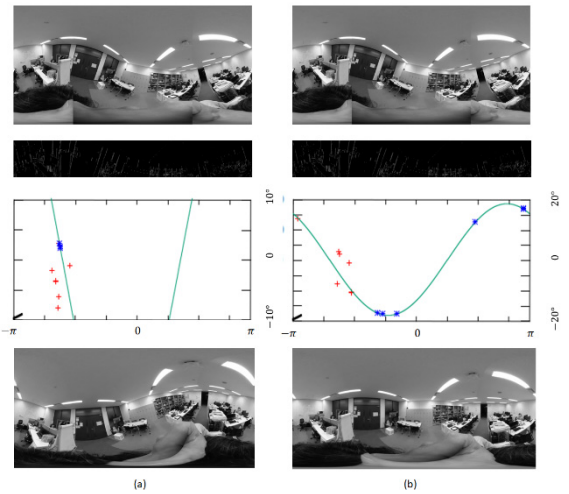

Figure 13: Case in which the camera inclination is larger than *maxangle*.

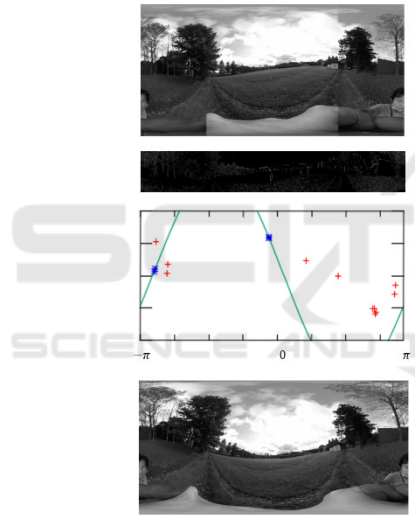

Figure 14: Failed examples of upright adjustment.

as short 2D curves, and the inclination can be corrected although the number of detected lines is smaller than that for the corridor. Figure 12(c) was taken in an elevator hall. It can be seen that the camera is tilted more than *maxangle* degrees, so almost half of the 3D lines are not detected, but the out-of-range camera tilt has been detected. As shown in Figures 12(d) and (e), the inclination correction can be performed stably outside a building. Figure 12(f) shows an image of a road far from buildings, but the inclination can be corrected by detecting street lights and signs and decreasing *pthresh*. The red line in the frame of the corrected image is (100-*pthresh*) thick, which visualizes the uncertainty of the estimation.

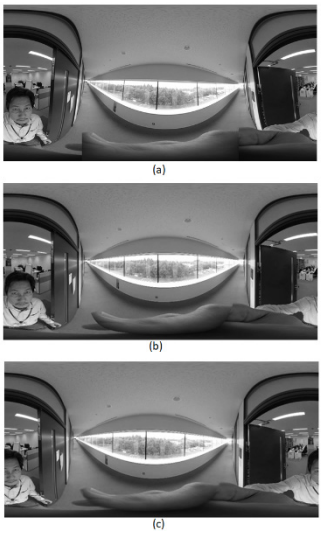

Figure 15: Comparison with the result obtained by the application of a camera manufacturer.

In Figure 13(a), because the camera is severely inclined, most of the projected curves of the 3D vertical lines are not detected with an inclination of more than *maxangle*, and since *pthresh* is reduced to 120, many incorrect lines are detected and the correction fails. Figure 13(b) shows a result of upright adjustment with a *maxangle* of 20°. When *pthresh* is 150, a straight line greater than *topthresh* can be detected, and the zenith direction can be correctly estimated even if an incorrect straight line is included in the RANSAC processing.

Figure 14 is an image at the edge of a field, and the zenith estimation fails because of the influence of a tree that extends obliquely across the few vertical lines that can be observed.

Figure 15(a) is a panoramic image before correction, Figure 15(b) is the result of adjustment obtained by the proposed method, and Figure 15(c) is the result obtained by an application from a camera manufacturer. The difference in correction accuracy can be seen around the door of the room.

A sample movie is also attached; the lower left is input, upper left is the image corrected by the proposed method with *maxangle* = 10, the upper right is the image corrected by the proposed method with *maxangle* = 20 and lower right is the image corrected by the manufacturer's application.

5.2 Estimation Accuracy

To evaluate the accuracy of camera inclination estimation, it is almost impossible to obtain ground truth with an accuracy of 0.1° because recent

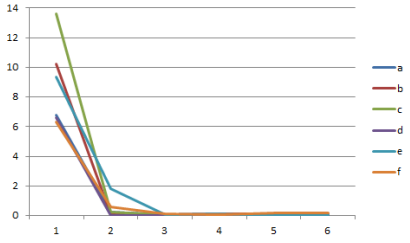

Figure 16: Corrected inclination for each iteration.

omnidirectional cameras are very small and there is little rigidity between the camera housing and image plane. Instead, we repeatedly performed the proposed upright adjustment to demonstrate the precision of our method. Figure 16 shows the results for the panoramic images of Figure 12. The number is the corrected angle for each iteration. Except for Figures 12(e) and (f), the corrected angles after the second iteration are smaller than 0.3°. This indicates that the camera inclination estimation accuracy of the proposed method is 0.3° when enough 3D vertical lines with adequate length are projected onto the panoramic images.

5.3 Consideration of Parameters

The parameters of the Hough transform are *maxangl*, *sampangle*, and *vertarea*. If the inclination of the camera can reach 30° , the *maxangle* may be set to about 2/3 thereof, and *sampangle* may be set equal to the estimation accuracy. In the previous processing example, *vertarea* = 300, which corresponds to an elevation angle of about −30° to 30° when the camera is not tilted. When the image size is changed, *vertarea* may be set accordingly. However, if a vertical line is far from the camera, the floor and ceiling are included, which is wasteful. It seems that the processing efficiency could be improved if *vertarea* were changed according to the environment and the height of the camera.

The parameters for line detection are *pthresh*, *topthresh,* and *dec*, and the parameters for RANSAC are *seednum* and *thinlier*. In the previous example, *pthresh* = *vertarea*/2, *topthresh* = 10, *dec* = 10, *seednum* = 3, and *thinlier* = 2 were empirically set, but good results have been obtained in various indoor and outdoor environments, and the settings may be varied accordingly.

5.4 Examination of Processing Speed

Table 1 shows the average time taken to execute parts ① to ⑤ in Figure 10. The first three columns on the left are the results for 3840×1920 panoramic images

Table 1: Processing speed.

	Before speed-up	After speed-up of ②	After speed-up	After speed-up for small image
①	16.1	16.2	20.3	3.9
②	459.4	33.1	7.7	1.0
③	7.3	5.2	8.2	1.0
④	0.1	0.1	0.2	0.1
⑤	783.8	772.5	96.5	12.1
Sum	1266.7	827.1	132.9	18.1

unit: msec

and the rightmost column shows the results for 1280×720 panoramic images. The processor was a Core i7-8850H and the operating system was Ubuntu18.04. The first column shows the result before speedup. In the second column, the processing speed was increased by tabulating ② and the processing time was reduced to about 1/15 the original time. The result in the third column, obtained after OpenMP acceleration, is a total time of about 133 ms, which can enable real-time processing at around 5 fps. For the small image, the total time is about 18 ms, and real-time processing at a camera frame rate of 15 fps was realized.

6 COMPARISON WITH A SIMILAR METHOD

In the method of (Kawai 2019) (A) introduced in Section 2, the edge image of a panoramic image is created, a block of edge points extending in the longitudinal direction near the vertical center is selected, and a straight line is detected by a conventional Hough transformation. Next, (ω, α) groups are determined, and a sine wave is used to estimate the inclination of the camera and correct the image inclination. This approach is the same as the approach of the proposed method, but the proposed method (B) has the following advantages.

In A, the longitudinal line is detected by the Hough transform as described above, but in B, a theoretical formula for the projection curve of a 3D straight line is derived. A 3D straight line is detected by the Hough transform using this formula, so that edge points far away from the vertical center can also be used.

In A, the hypothesis that the change in inclination in the width direction is periodic and can be approximated by a sine wave is introduced from the observation of a group of vertical straight lines detected near the vertical center on the panoramic image. In B, however, an equation for the inclination of a group of parallel straight lines on the vertical

center on the panoramic image is derived. It was shown analytically that the inclination may be approximated by a sine wave.

In A, the sine wave is fitted by the least squares method, whereas in B, robust and accurate fitting is realized by eliminating outliers using RANSAC.

In A, the estimation accuracy is 3.3° for the first correction and 1.5° for the second one, but in B, an estimation accuracy of 0.1° is obtained without the need for a second step (when the effect of noise can be eliminated).

For A, it was reported that there were no failure examples in an experiment of 40 examples, but only one example was shown. For B, many experiments were carried out in various environments, and concrete examples are shown.

7 CONCLUSIONS

In this paper, we proposed a method for upright adjustment of a panoramic image by detecting the inclination of the camera from a pre-corrected panoramic image with high accuracy and at high speed using a vertical line existing in an indoor environment or an outdoor environment near a building.

Because of the nature of this method, it cannot be used in an environment without vertical lines, but it is useful in many environments in which autonomous robots are expected to operate in the future, such as normal indoor environments, construction sites, and in and around warehouses. When the lengths of the projection curves are extremely short, the method is easily affected by noise, and the upright adjustment tends to be unstable. However, even in this case, the value of *pthresh* can be added as a certainty and the correct handling can be performed in the post-processing.

In future, this method will be applied to tasks such as the self-localization of autonomous robots, reconstruction of 3D environments, and object recognition. In addition, by integrating self-localization estimation and a 3D environment model, speed-up and robustness will be achieved by learning the parameters of the upright adjustment depending on location.

REFERENCES

Bazin, J.-C., Demonceaux, C., et al. 2012. Rotation estimation and vanishing point extraction by omnidirectional vision in urban environment. *The International Journal of Robotics Research* 31(1): 63-81.

Bosse, M., Rikoski, R., et al. 2002. Vanishing points and 3d lines from omnidirectional video. *Proceedings. International Conference on Image Processing*, IEEE.

Canny, John 1986. A computational approach to edge detection. *IEEE Transactions on Pattern Analysis and Machine Intelligence*, 8(6): 679-698.

Cipolla, R., Robertson, D., et al. 1999. Photobuilder-3D models of architectural scenes from uncalibrated images. *Proceedings IEEE International Conference on Multimedia Computing and Systems*, IEEE.

Coughlan, J. M. and Yuille, A. L. 1999. Manhattan world: Compass direction from a single image by bayesian inference. *Proceedings of the seventh IEEE international conference on computer vision*, IEEE.

Demonceaux, C., Vasseur, P., et al. 2006. Omnidirectional vision on UAV for attitude computation. *Proceedings 2006 IEEE International Conference on Robotics and Automation, 2006. ICRA 2006.*, IEEE.

Demonceaux, C., Vasseur, P., et al. 2007. UAV attitude computation by omnidirectional vision in urban environment. *Proceedings 2007 IEEE International Conference on Robotics and Automation*, IEEE.

Fischler, A., Martin and Bolles, C., Robert 1981. Random sample consensus: a paradigm for model fitting with applications to image analysis and automated cartography. *Communications of the ACM*, 24(6): 381-395.

Gallagher, A. C. 2005. Using vanishing points to correct camera rotation in images. *The 2nd Canadian Conference on Computer and Robot Vision (CRV'05)*, IEEE.

Illingworth, John and Kittler, Josef 1988. A survey of the Hough transform. *Computer vision, graphics and image processing*, 44(1): 87-116.

Jayasuriya, M., Ranasinghe, R., et al. 2020. Active Perception for Outdoor Localisation with an Omnidirectional Camera. *IEEE/RSJ International Conference on Intelligent Robots and Systems*.

Jeon, J., Jung, J., et al. 2018. Deep Upright Adjustment of 360 Panoramas Using Multiple Roll Estimations. *Asian Conference on Computer Vision*, Springer.

Joo, K., Oh, T.-H., et al. 2018. Globally optimal inlier set maximization for Atlanta frame estimation. *Proceedings of the IEEE Conference on Computer Vision and Pattern Recognition*.

Jung, J., Kim, B., et al. 2017. Robust upright adjustment of 360 spherical panoramas. *The Visual Computer* 33(6-8): 737-747.

Jung, R., Lee, A. S. J., et al. 2019. Deep360Up: A Deep Learning-Based Approach for Automatic VR Image Upright Adjustment. *2019 IEEE Conference on Virtual Reality and 3D User Interfaces (VR)*, IEEE.

Kawai, N. 2019. A method for rectifying inclination of panoramic images. *ACM SIGGRAPH 2019 Posters*, ACM.

Lee, H., Shechtman, E., et al. 2013. Automatic upright adjustment of photographs with robust camera

calibration. *IEEE Transactions on Pattern Analysis and Machine Intelligence* 36(5): 833-844.
Liu, M., Pradalier, C., et al. 2013. Visual homing from scale with an uncalibrated omnidirectional camera. *IEEE transactions on robotics* 29(6): 1353-1365.
Milford, M. and Wyeth, G. 2010. Persistent navigation and mapping using a biologically inspired SLAM system. *The International Journal of Robotics Research* 29(9): 1131-1153.
Natraj, A., Ly, D. S., et al. 2013. Omnidirectional vision for UAV: Applications to attitude, motion and altitude estimation for day and night conditions. *Journal of Intelligent & Robotic Systems* 69(1-4): 459-473.
Payá, L., Gil, A., et al. 2017. A state-of-the-art review on mapping and localization of mobile robots using omnidirectional vision sensors. *Journal of Sensors* 2017.
Ricoh. 2020. "Theta." from https://theta360.com/en/.
Schindler, G. and Dellaert, F. 2004. Atlanta world: An expectation maximization framework for simultaneous low-level edge grouping and camera calibration in complex man-made environments. *Proceedings of the 2004 IEEE Computer Society Conference on Computer Vision and Pattern Recognition, 2004. CVPR 2004.*, IEEE.
Wang, C., Tanahashi, H., et al. 2003. Slant estimation for active vision using edge directions in omnidirectional images. *Proceedings 2003 International Conference on Image Processing (Cat. No. 03CH37429)*, IEEE.
Xiao, J., Ehinger, K. A., et al. 2012. Recognizing scene viewpoint using panoramic place representation. *2012 IEEE Conference on Computer Vision and Pattern Recognition*, IEEE.
Yagi, Y. 1999. Omnidirectional sensing and its applications. *IEICE transactions on information and systems* 82(3): 568-579.
Zhang, L., Lu, H., et al. 2016. Vanishing point estimation and line classification in a Manhattan world with a unifying camera model. *International Journal of Computer Vision* 117(2): 111-130.